18th European Symposium on Computer Aided Process Engineering – ESCAPE 18
Bertrand Braunschweig and Xavier Joulia (Editors)

Large-Scale Nonlinear Programming Strategies for the Operation of LDPE Tubular Reactors

Victor M. Zavala and Lorenz T. Biegler

Department of Chemical Engineering, Carnegie Mellon University, 5000 Forbes Avnue, Pittsburgh PA 15213, USA

Abstract

There is substantial economic interest to optimize the operations of low-density polyethylene (LDPE) tubular reactors. Due to the high complexity of these units, systematic optimization techniques need to be used for this. One of the main limitations associated to this is the high dimensionality and complexity of the multi-zone tubular reactor model. In this work, we demonstrate that a simultaneous full-discretization approach coupled to a full-space nonlinear programming (NLP) solver results in an efficient strategy to cope with these limitations. We exploit these advantages in the analysis of different scenarios arising in the operation of LDPE reactors. In particular, we propose a multivariable optimization strategy able to compensate for time-varying disturbances in order to keep the reactor temperature profile and final properties of the polymer at targets. Finally, we show that the optimizer can easily be extended to incorporate economic decisions in the objective and we illustrate the potential benefits and bottlenecks of this approach.

Keywords: LDPE, tubular reactor, large-scale optimization, operations, economics.

1. Introduction

Low-density polyethylene (LDPE) is often produced in tubular reactors through free-radical polymerization of ethylene at high pressures (1500-3000 atm) and in the presence of peroxide initiators. In addition, a chain-transfer agent (CTAs) is incorporated in order to control the polymer melt index. While LDPE processes are often highly profitable, there exist multiple factors limiting their performance. The high exothermicity of the reactions and the high pressures force the design of long multi-zone tubular reactors (1-3 km) with thick walls, small inside diameters (6-10 cm) and sophisticated jacket cooling systems. A schematic representation of a typical LDPE reactor is presented in Figure 1. These designs involve multiple peroxide, monomer and CTA side streams distributed along the reactor zones. This gives rise to strong multivariable interactions between different phenomena occurring downstream of the reactor and leads to complex operating procedures. In addition, the selected operating conditions might also promote continuous polymer deposition on the reactor walls (fouling) that further limit the reactor productivity (Buchelli et.al, 2005).

During the last years, several steady-state rigorous models for LDPE tubular reactors have been proposed (Kiparissides et.al, 2005). These models usually comprise several hundred highly nonlinear differential and algebraic equations (DAE) that describe the evolution of the reacting mixture along the reactor. In addition, in most reactor arrangements, the zone jackets are operated countercurrently, giving rise to multi-point boundary conditions. The resulting model complexity has limited the use optimization techniques, especially in on-line applications where fast solutions are required

(Asteuasin and Brandolin, 2007). In this work, we propose a full-discretization formulation of LDPE tubular reactor models. The strategy is able to handle multi-point boundary conditions along the reactor zones. In addition, it allows the use of efficient NLP solvers able to solve highly nonlinear problems with many degrees of freedom quickly and efficiently. These benefits are exploited in the design of a multivariable optimizer for LDPE reactors that can be used for different operating scenarios of industrial interest.

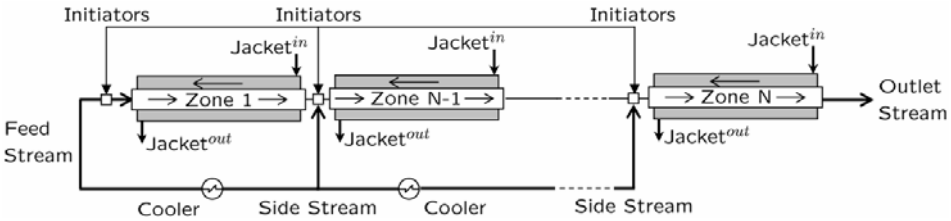

Figure 1. Schematic representation of multi-zone LPDE tubular reactor.

2. Mathematical Model

2.1. Model Structure

In this work, we consider the rigorous model presented in (Zavala and Biegler, 2006). The model describes the steady-state evolution of the reacting mixture and of the cooling agent along each one of the reactor zones. The material balance equations have the generic form,

$$\begin{aligned} &\frac{1}{A_k}\frac{dF_{k,j}}{dz} = r_{k,j}(z_k) \quad k=1,...,N,\ j=1,...,NS \\ &F_{k,j}(0) = \varphi_k^M\left(F_{k-1,j}\left(z_{k-1}^L\right), F_{k,j}^{ss}\right) \quad k=2,...,N,\ j=1,...,NS \\ &F_{1,j}(0) = F_j^{fs} \quad j=1,...,NS \end{aligned} \tag{1}$$

Where $F_{k,j}$ denotes the molar flow rate of component j at zone k and $r_{k,j}$ denotes the corresponding net reaction rate varying along the axial position z_k at each zone. The components present in the mixture are the multiple peroxides contained in the initiator feed streams, monomer, comonomer, solvent, chain-transfer agent(s), moments of live polymer chains, moments of dead polymer chains, long-chaing branching and short-chain branching. Symbols N and NS denote the number of reactor zones and species in the mixture, respectively. $F_{k,j}^{ss}$ denotes the side stream flowrate of a particular component to a particular zone while F_j^{fs} denotes the feed stream flowrate of a particular component. Finally, A_k is the internal cross-sectional area of a given zone, z_k^L is the corresponding total length. Symbol $\varphi_k^M(\cdot)$ denotes material balances at the feed points which implicitly determine the initial conditions of the zones. The model incorporates energy balances for the reacting mixture along the zones,

$$\rho_k^R(z_k)v_k^R(z_k)C_{p,k}^R(z_k)\frac{dT_k^R}{dz} = r_p - \frac{4U_k}{d_k}\left(T_k^R(z_k) - T_k^J(z_k)\right) \quad k=1,...,N$$

$$T_k^R(0) = \varphi_k^R\left(F_{k-1,j}\left(z_{k-1}^L\right), T_{k-1}^R\left(z_k^L\right), F_{j,k}^{ss}, T_k^{in}\right) \quad k = 2,..., N$$
$$T_1^R(0) = T_1^{in} \tag{2}$$

Where ρ_k^R, ν_k^R and $C_{p,k}^R$ are the density, velocity and heat capacity of the reacting mixture, respectively, which vary along the axial position. Symbol d_k denotes the zone diameter. Functions $\varphi_k^R(.)$ denote energy balances at the feed points. For the cooling agent flowing along the jackets we have the energy balances,

$$\rho_k^J(z_k)\nu_k^J(z_k)C_{p,k}^J(z_k)\frac{dT_k^J}{dz} = -\frac{\pi d_k U_k}{A_k^J}\left(T_k^J(z_k) - T_k^R(z_k)\right) \quad k = 1,..., N$$
$$T_k^J\left(z_k^L\right) = T_k^{in} \quad k = 1,..., N \tag{3}$$

where ρ_k^J, ν_k^J and $C_{p,k}^J$ are the density, velocity and heat capacity, respectively, of the cooling agent which vary along the axial position. From (3) notice the presence of boundary conditions that dictate the inlet temperature of the cooling agent at the end of the reactor zone. The reactor model includes a large number of algebraic equations for the calculation of the thermodynamic, physical, and transport properties of the reacting mixture and of the polymer molecular properties (molecular weights, branching, melt index and polymer density). The reactor model used in this work contains around 130 ordinary differential equations and 500 algebraic equations; these are fully described in Zavala and Biegler (2006).

2.2. Model Uncertainty

There exists a high degree of uncertainty in the model associated to the heat transfer coefficients (HTCs) of the zones, which originates from the time-varying fouling layer inside the reactor encountered in industrial operations. It has been so far impractical to incorporate mechanistic models to predict this fouling onset (Buchelli, et.al, 2005). A typical strategy to get around this limitation consists in parameterizing the HTCs and estimating them on-line. The HTCs are estimated to match the reactor temperature profile and the jacket temperatures. In a previous study (Zavala and Biegler, 2006), we proposed an on-line estimation strategy able to match the temperature profile accurately. The strategy follows a simultaneous all-at-once approach to match the entire reactor and jacket temperatures. In Figure 2 we illustrate the resulting match of the reactor temperature profile at a particular point in time.

3. NLP Formulation and Solution

After embedding the rigorous reactor model to a general objective function and inequalities, we obtain a DAE-constrained optimization problem. In this work, the optimizer is allowed to manipulate some of the reactor inputs (initiator flows, jacket flowrates, CTA flowrates and side feed temperatures) all at once. The novelty of the approach lies on the multivariable all-at-once nature of the strategy which accounts for downstream interactions along the reactor. This is in sharp contrast with the current industrial practice where individual loops are used to control *locally* the reactor zones peak, inlet and outlet temperatures which complicate the control of the polymer properties at the reactor exit. The proposed strategy is expected to decouple these control loops and thus obtain better performance.

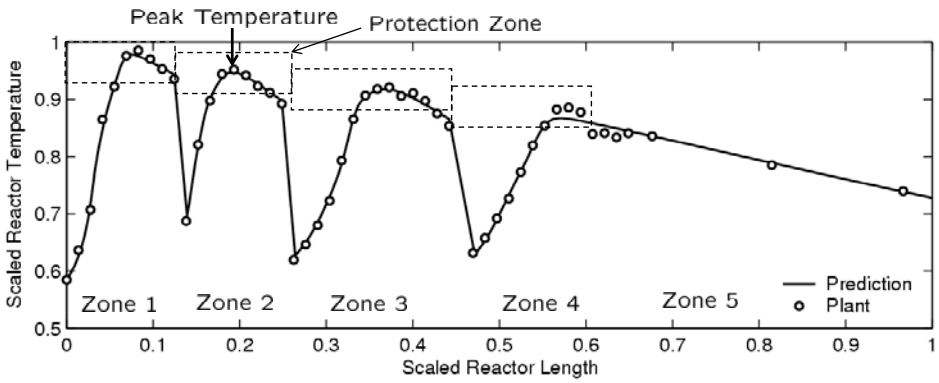

Figure 2. Reactor model match of temperature profile after estimation of HTC and initiator efficiencies.

We propose a simultaneous full-discretization approach to solve the DAE-constrained problem. A Radau collocation scheme is used in order to incorporate, directly, the multi-point boundary conditions. After discretization, we obtain an NLP with around 13,000 constraints and 71 degrees of freedom. The resulting NLP is very sparse and this structure can be exploited using the full-space interior point solver IPOPT. The NLP is implemented on the modeling platform AMPL which provides exact first and second order derivative information. This information is important in order to handle highly nonlinear NLPs. On average, the NLPs converge in around 10-12 iterations and 15-20 CPUs on a Pentium IV, 3.0 GHz PC.

4. Case Studies

4.1. Tracking Objective Function

In the first case study, we evaluate the performance of the optimizer for a given decaying sequence of the HTC in the reaction zones. This scenario arises during normal operation where the HTC drops from its original value after the defouling or cleaning stage (Buchelli, et.al, 2005). The simulated decreasing HTC sequence for the reaction zones is illustrated in Figure 3. The HTC is ramped linearly from its nominal value (value of 1) to less than 40% of its nominal value. The nominal point is obtained by matching the reactor model to industrial plant data. The optimizer objective is to react to the changing HTCs by manipulating the full set of input variables in order to keep the reactor peak temperatures within the protection zones (see Figure2) and the polymer properties on target. For confidentiality reasons, all the variables have been scaled using their nominal values. The plant response is obtained by perturbation of the heat transfer coefficients in the simulation model.

The resulting input profiles of the optimizer are presented in Figure 4. It is clear that, as the HTC decays (i.e., the reactor fouls) the controller can only keep the reactor under the desired peak temperature limits by dropping production (-12% in the most fouled case). This is normally done by decreasing the initiator flows in the zones independently. However, it is interesting to observe that the optimizer decides to move only the initiator of the first (Z1) and second (Z2) reaction zones while the flows for Z3 and Z4 are kept at their nominal values. In Z3 and Z4 the optimizer decides that it is more efficient to attenuate the decreasing cooling capacity by decreasing the feed temperatures at the mixing points. Also, the optimizer is able to keep the melt index and

polymer density always on target despite of the decreased conversion. For this, the optimizer drops the CTA side flowrates at the same rate in all zones. From the temperature profile, it is possible to observe that the fouling onset is most notable in the first reaction zone where the outlet temperature tends to rise; the optimizer manipulates the feed temperature to the second reaction zone to keep the inlet temperature of this zone at target.

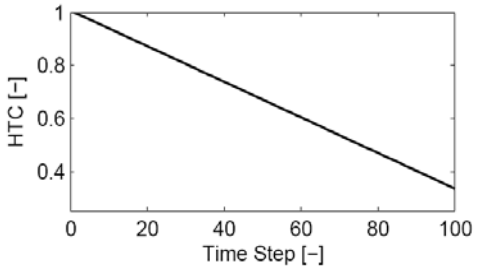

Figure 3. Decaying sequence for heat transfer coefficients along all reaction zones.

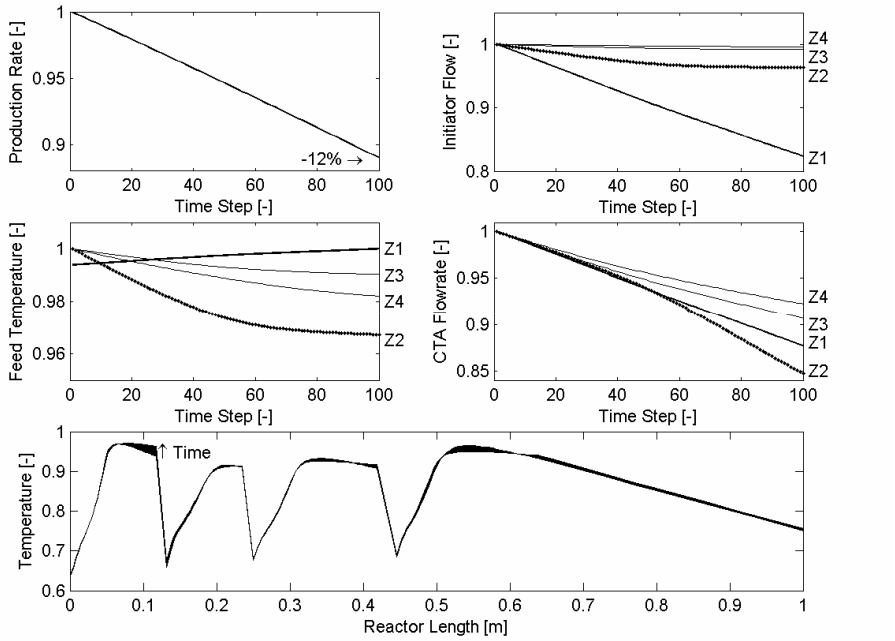

Figure 4. Response of optimizer to decaying sequence of HTCs in reaction zones.

Case 2.2. Tracking Objective Function + Economic Objective

In this case, we incorporate an additional term in the objective function to maximize production. From Figure 5, it is clear that the incorporation of the economic term in the objective forces the optimizer to manipulate the inputs in order to attenuate the decreased production. In this case, the optimizer only needs to drop production by 7% in the most fouled case (saving 5% compared to first case study). Furthermore, for the highest value of the HTC, the optimizer is able to increase production by 3%. Interestingly, the optimizer keeps the same trends of the initiator flowrates as in the previous case study. In this case, the optimizer overcomes the lost production due to

fouling by decreasing the feed temperatures. This increases the temperature difference between the inlet and the peak temperatures, thus increasing production. Finally, the melt index and density are always kept at target. For this, the CTA flowrate profiles need to be distributed in a different way compared to the previous case study. It is important to emphasize that, even if the multivariable optimizer can attenuate the lost production by distributing the inputs more efficiently, it is not able to overcome the lost production completely. As expected, this implies that production losses are dominated by the fouling effect.

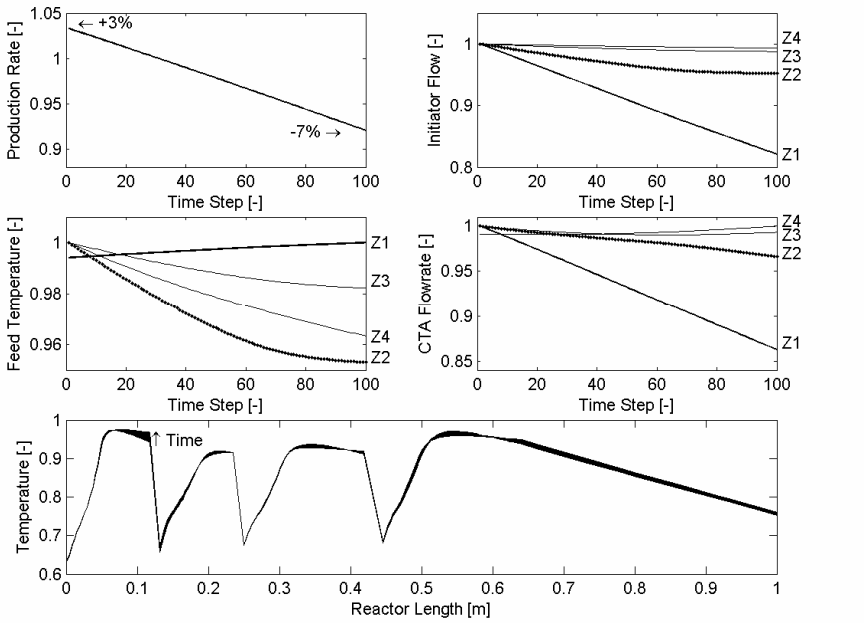

Figure 5. Response of optimizer to decaying sequence of HTCs in reaction zones. Economics included in objective function.

5. Conclusions and Future Work

In this work, we propose an all-at-once discretization strategy to optimize the operations of LDPE processes using first-principles tubular reactor models. It is demonstrated that the multivariable strategy can cope rigorously with downstream interactions along the reactor and attenuate disturbances in order to follow objectives of industrial interest. As part of future work, we will incorporate rigorous dynamic models that will allow for a higher fidelity in the analysis.

References

A. Buchelli et.al., 2005, Modeling Fouling Effects in LDPE Tubular Polymerization Reactors. 1. Fouling Thickness Determination, I&ECR, 44(5), 1474-1479.

C. Kiparissides et.al., 2005, Mathematical Modeling of Free-Radical Ethylene Copolymerization in High-Pressure Tubular Reactors, I&ECR, 44(8), 2592-2605.

M. Asteuasin and A. Brandolin, 2007, Modeling and Optimization of a High-Pressure Ethylene Polymerization Reactor Using gPROMS, C&CE, In Press.

V. Zavala and L.T. Biegler, 2006, Large-Scale Parameter Estimation in Low-Density Polyethylene Tubular Reactors, I&ECR, 44(23), 7867-7881.